



# HIGH STRAIN RATE PROPERTIES OF AN $\text{SiC}_w/2124\text{-T6}$ ALUMINUM COMPOSITE AT ELEVATED TEMPERATURES

M. Guden and I.W. Hall\*

Izmir Institute of Technology, Basmane, Izmir 35230, Turkey

\*Mechanical Engineering Department and Materials Science Program,  
University of Delaware, Newark, DE 19716, USA

(Received February 10, 1998)

## Introduction

Metal matrix composites, (MMC's) provide several important advantages over unreinforced metals and alloys. Among these, higher moduli and yield stresses and enhanced thermo-mechanical properties are normally considered important in structural applications of MMC's. It is also possible that MMC's may be exposed to loading conditions involving high strain rates during service, for example, components of a car in collision with another or turbine blades hit by ingestion of foreign objects. In such situations of rapidly increasing loading conditions, the material property response may be considerably different from that which applies during slow loading of normal quasi-static testing and, consequently, dynamic mechanical properties are of increasing interest and importance.

Several studies involving dynamic deformation of a  $\text{SiC}_w/2124\text{-T6}$  Al MMC have already been conducted using tension [1], shear [2], compression [3] and projectile impact [4] testing. The purpose of the present study was to extend the high strain rate data to include high temperature effects. Mechanical test results and microstructural observations of features of dynamic deformation have been compared with data from the unreinforced alloy to obtain more complete information on the dynamic response of the composite.

## Materials and Experimental

The  $\text{SiC}_w/2124\text{-T6}$  composite was in the form of plate, 6.4 mm in thickness, and contained 25V<sub>f</sub>% SiC whiskers in a 2124-T6 Al matrix alloy. The whiskers were 2 to 10  $\mu\text{m}$  in length with a diameter of 0.1–0.5  $\mu\text{m}$  and the composite was manufactured by a powder metallurgy route involving hot consolidation, extrusion and cross-rolling. Reinforcement distribution in the MMC was observed to be slightly aligned in the extrusion direction. Compression testing was performed normal to the rolling plane. Unreinforced 2024-T6 alloy (practically identical in composition to 2124) was also obtained in the form of 6.3 mm thick rolled plate. The average grain size of the unreinforced alloy was determined by optical microscopy to be  $\sim 180 \mu\text{m}$  while that of the composite was smaller at  $\sim 10 \mu\text{m}$ .

High strain rate and quasi-static compression tests were conducted on small (6.3 mm in length and 8.3 mm in diameter) cylindrical specimens of composite and unreinforced alloy using a compression type Split Hopkinson Pressure Bar (SHPB) apparatus and a screw driven Instron machine. Details of the specific SHPB used and data reduction are given elsewhere [5]. A small, split-tube furnace covering the

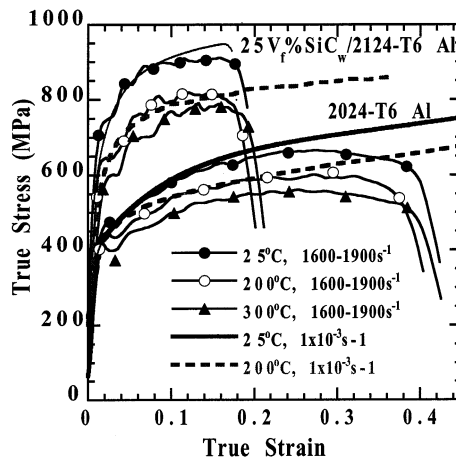


Figure 1. True stress/true strain curves for MMC (top 5 curves) and matrix (lower 5 curves) as functions of temperature and strain rate.

specimen and only a small portion of the bars was used to conduct high temperature tests in the SHPB. The furnace, together with the bars, was heated to the desired temperature, the specimen was placed between the bars and a soaking time of 5 minutes was allowed. Data correction for the resulting temperature gradient was made after the procedure given by Lindholm [6].  $\text{MoS}_2$  oil-based lubricant was used to reduce friction effects at room temperature and graphite powder was used for high temperature tests.

### Results

Typical high strain rate compression behaviors of the composite and unreinforced alloy at 25°, 200° and 300°C are shown in Fig. 1 along with quasi-static stress strain curves at 25° and 200°C. In quasi-static testing at 25°C, composite samples fractured at strains of 15 to 20% while unreinforced alloy samples did not fracture until ~70% strain. At higher temperatures and quasi-static strain rates unreinforced alloy samples deformed plastically until strains in excess of 50% without failure and composite samples showed fracture strains of ~40% strain, more than twice the corresponding room temperature fracture strain (~15%), although cracks were observed on the side of the samples. However, it was found that at dynamic strain rates neither the composite nor the unreinforced alloy samples showed any significant increase in ductility with increasing test temperature. At 200° and 300°C both the dynamic and quasi-static flow stress values for composite and unreinforced alloy decreased as expected. Also, it should be noted that, relative to quasi-static rates, there was a gradual decrease of flow stress with increasing strain at dynamic strain rates for both materials at all temperatures.

Since adiabatic heating effects become increasingly important at large strains and because the SHPB is inherently unable to measure flow stresses accurately at small strains, the strain rate sensitivity of flow stress is generally determined at an intermediate, constant strain value: 5% strain is used in this study. In Fig. 2, values of flow stress at 5% strain are shown as a function of strain rate for composite and unreinforced alloy at 25° and 200°C. At both temperatures the composite and unreinforced alloy are found to be strain rate insensitive at 5% strain. Note, however, that the composite shows a ~100 MPa decrease in flow stress between 25° and 200°C while the unreinforced alloy shows only a ~50 MPa decrease.

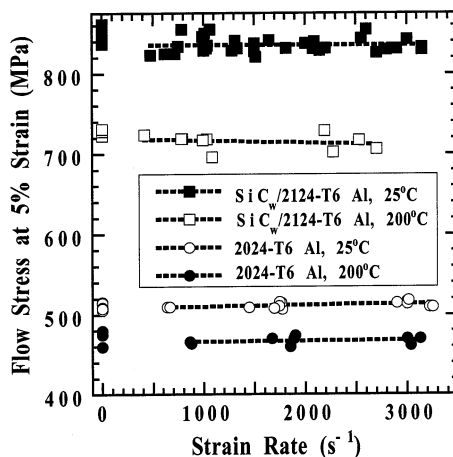


Figure 2. Flow stress at 5% strain vs. strain rate at 25° & 200°C.

Fracture in both materials always occurred by shear band formation on a plane at  $\sim 45^\circ$  to the loading direction, the plane of maximum shear stress in compressive loading, and was preceded by cracking and void formation at particles along the band, as shown in Fig. 3 for the unreinforced alloy. Final failure was by coalescence of these cracks/voids. In the shear band region, grains are highly distorted, Fig. 4, and showed a dramatic change in orientation near the fracture surface. The inset to Fig. 4 shows schematically the usual mode of fracture: fragments 1 and 2 were identical and shear banding occurred in region 'A'. Fig. 5(a) is a TEM micrograph of a section through a partially formed shear band in unreinforced alloy clearly showing the large strain experienced. Preferential electropolishing around the grain boundary particles has highlighted the particles which nucleate voids there. Nevertheless, Fig. 5(b) shows that, despite the large strain, negligible void formation has occurred.

As an approximation, the shear band width may be calculated from the area where grain orientation became almost parallel to the shear band and it was found to be approximately 25 and 40  $\mu\text{m}$  at 25° and 300°C, respectively. The strain in the band can also be calculated and shown to be in the range 100–300% very near to the band, corresponding to a local strain rate value of  $10^5$  to  $10^6$   $\text{s}^{-1}$ . Since the grain and whisker sizes in the MMC are very small and the shear band region is narrow and formed in

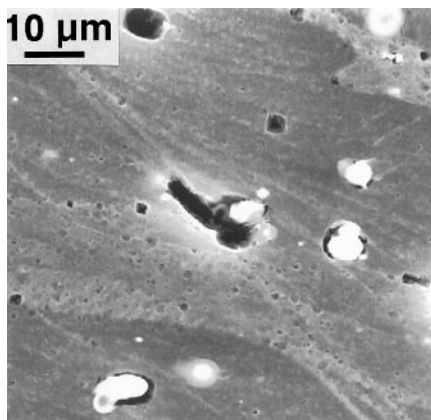


Figure 3. Void formation at particles in shear band.

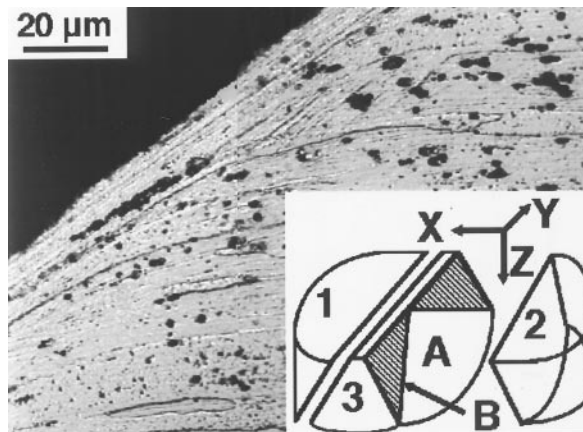


Figure 4. Optical micrograph showing change in grain orientation adjacent to shear band and schematic diagram of typical fracture mode.

a few microseconds, the bands are not as well defined or as easily detected as in the case of unreinforced alloy. However, fractured samples cut from the X-Z plane of Fig. 4 have shown that, in a narrow region near the fracture surface, whiskers are aligned through the fracture surface showing rotation of whiskers along the band. Observations show that the shear band regions in the composite were narrower than those of unreinforced alloy and were 5 and 15  $\mu\text{m}$  at 25°C and 300°C, respectively.

In unreinforced alloy, region 'A' (inset of Fig. 3) consisted of elongated dimples, Fig. 6, but much of the surface was smeared out due to sliding of mating fracture surfaces. Similar to the unreinforced alloy, fracture in the composite occurred in the shear band region. Typical fracture surfaces also exhibited the same regions, A & B, as in the case of unreinforced alloy except for samples tested at 200°C at quasi-static strain rates. In these samples the fracture strains were higher than 40% and the fracture surfaces mostly consisted of ductile regions. Fig 7 shows a typical composite fracture surface corresponding to region A in which whiskers are seen to have been aligned normal to the fracture surface, indicating a tensile opening mode in this region.

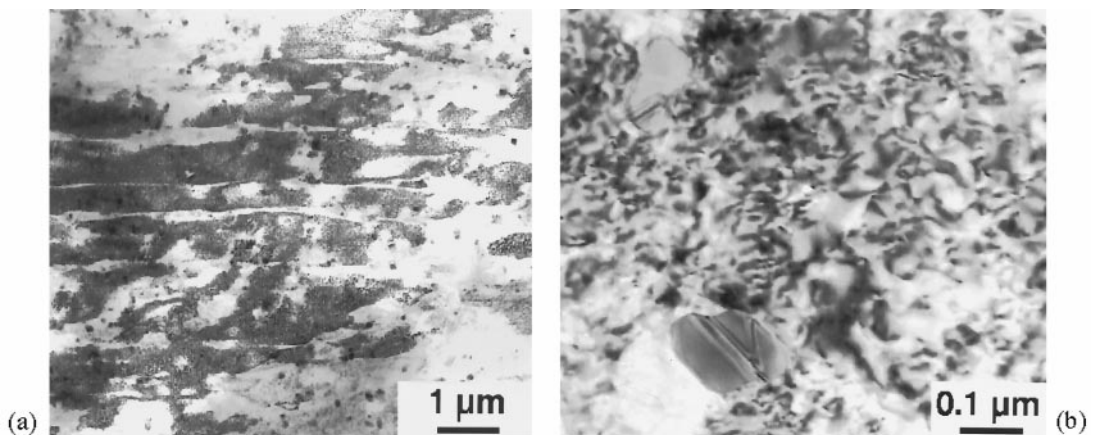


Figure 5. (a) TEM micrograph of shear band showing heavily deformed subgrains. Fig. 5(b) Center of shear band showing uniform dislocation generation, particles and no voids.

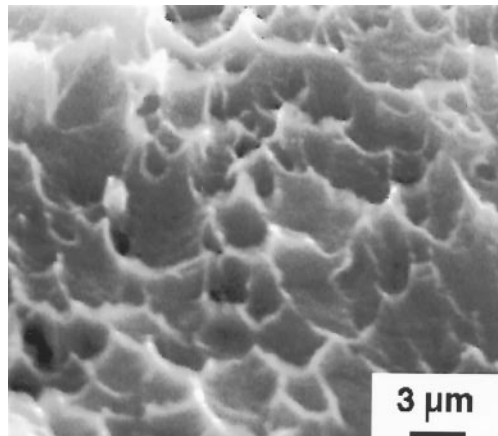


Figure 6. Fracture surface of unreinforced alloy showing elongated ductile dimples.

### Discussion

It has been shown that the unreinforced alloy and composite exhibit strain rate insensitive flow stress behavior, in agreement with previous reports for similar unreinforced and composite materials [2, 7]. Moreover, the present study has clearly shown that both materials are still rate insensitive at 200°C and available data indicate that this is also true at 300°C. One of the proposed mechanisms for flow stress rate sensitivity in metallic materials is thermally activated dislocation/obstacle interaction. The absence of rate sensitivity in 2024-T6, therefore, indicates that these mechanisms are of minor importance and that athermal stresses dominate the high temperature behavior.

The reduced flow stresses at high strain rates and large strains compared to quasi-static strain rates may be explained by considering the thermal softening and shear localization effects which occur at high strain rates. The observed increased regions of ductile fracture surface of the samples are in good agreement with the above rationale since strain rate can prompt very high temperatures and large strains in the band. Adiabatic shear band formation in similar MMC's and unreinforced alloys was reported previously. The shear band thicknesses were reported to be 20–30  $\mu\text{m}$  and 5–10  $\mu\text{m}$  for 7 and 20V<sub>f</sub>%

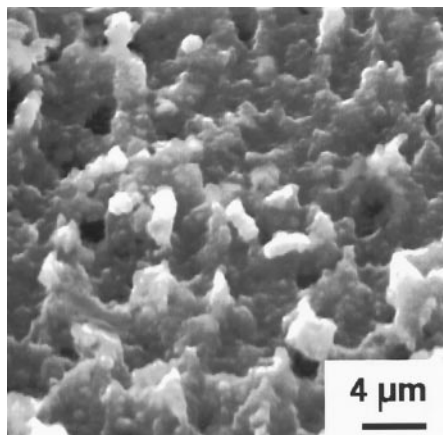


Figure 7. Fracture surface of MMC showing whisker “pull-out” and matching holes.

SiC<sub>w</sub>, respectively [4]. Leech [8] conducted projectile impact on 7039 Al and observed adiabatic shear band thicknesses of 20  $\mu\text{m}$ . Woodward *et al.* [9] carried out compression drop tests on 2024-T351 Al alloy at quasi-static and high strain rates. Reduced flow stresses and ductility at high strain rates compared to quasi-static strain rates were observed and were attributed to thermal softening and adiabatic shear band formation.

Even though the MMC and alloy showed a large increase in ductility in quasi-static compression tests at 200°C, there was no enhancement of ductility for either material at high strain rates as the test temperature increased, see Fig. 1. The temperature independent fracture strains of the composite and unreinforced alloy are, therefore, clear evidence that thermal softening and shear localization remain the dominant mechanisms limiting the mechanical deformation at high strain rates. The microscopic observations on fracture surfaces and polished surfaces of the deformed samples essentially prove that adiabatic shear band formation was the main damage process leading to relatively low ductility of the composite and unreinforced alloy at high strain rates.

Fig. 2 shows that the decrease in flow stress between 25° and 200°C is approximately 100 MPa and 50 MPa for the composite and alloy respectively. The difference is believed to be due to the reduced level of residual stress in the composite at the higher temperature. Arsenault and Shi [10] modeled the contribution to the yield stress arising from dislocations induced by the difference of coefficients of thermal expansion between matrix and reinforcement. Calculations using their model predict that on heating to 200°C, the contribution to the strength of the composite will be reduced by approximately 40 MPa compared with the room temperature strength. The more marked decrease for the composite is, therefore, a consequence of the reduction of thermal residual stresses at the higher temperature.

### Conclusions

It was found that, within the strain rate range investigated, both composite and unreinforced alloy exhibited essentially rate insensitive 5% flow stress values at 25° and 200°C. Tests at higher temperatures and high strain rates showed that both materials were prone to shear band formation over the studied temperature range. Microstructural observations of fracture and polished surfaces of the materials confirmed that severe deformation and subsequent fracture was largely confined to the region of the adiabatic shear bands. Ductile fracture together with smeared regions on the fracture surfaces were observed and corresponded well with previous observations.

The similarity between composite and unreinforced alloy in terms of mechanical properties and fracture mechanism provides strong supporting evidence for the dominating importance of the matrix properties in determining the response of MMC's to dynamic loading situations.

### Acknowledgments

Financial support from the Army Research Office (award #DAAH04-95-2-0001) and a fellowship (M.G.) from the Izmir Institute, Turkey, are gratefully acknowledged.

### References

1. J. Harding and M. Taya, in Proceedings of the ICCM-6/ECCM-2, p. 2.224, Elsevier Applied Science, Amsterdam (1987).
2. A. Marchand, J. Duffy, T. A. Christman, and S. Suresh, *Eng. Fract. Mech.* 30, 295 (1988).
3. A. Kalambur and I. W. Hall, *Scripta Mater.* 37, 193 (1997).
4. K. Cho, S. Lee, W. B. Choi, and I. Park, in *Advanced Composites '93*, International Conference on Advances in Composite Materials, ed. T. Chandra *et al.*, p. 1265, The Mining Metals & Materials Society (1993).

5. M. Guden and I. W. Hall, *Mater. Sci. Eng. A*, A232, 10 (1997).
6. U. S. Lindholm and L. M. Yeakley, *Exp. Mech.* Jan. 1, (1968).
7. S. I. Hong, G. T. Gray III, and J. J. Lewandowski, *Acta Metall. Mater.* 41, 2337 (1993).
8. P. W. Leech, *Metall. Trans.* 16A, 1900 (1985).
9. R. G. O'Donnell and R. L. Woodward, *J. Mater. Sci.* 23, 3578 (1988).
10. R. J. Arsenault and N. Shi, *Mater. Sci. Eng.* 81, 175 (1986).